J|A|C|S
COMMUNICATIONS

Published on Web 02/05/2005

Mixed Valence Isomers

J. Catherine Salsman and Clifford P. Kubiak*

Department of Chemistry and Biochemistry, University of California, San Diego, La Jolla, California 92093-0358

Tasuku Ito

Department of Chemistry, Tohoku University, Aoba, Aramaki, Aoba-ku Sendai 980-8578, Japan

Received December 20, 2004; E-mail: ckubiak@ucsd.edu

We report the direct spectroscopic observation of mixed valence isomers, the two alternate charge distributions of a mixed valence complex. In the normal two-state Marcus−Hush description of a symmetric mixed valence complex,[1,2] electron exchange is a degenerate process, and the "isomers", differing only in the position of the charge, cannot be distinguished. By introducing a slight asymmetry into a mixed valence complex, it is possible in principle to introduce a small energy difference between the two sides of the Marcus−Hush potential energy surface such that substantial Boltzmann populations of the two mixed valence isomers can exist in equilibrium. It appears that these conditions are seldom met. Energy differences between the mixed valence isomers are either too large to observe measurable amounts of the less stable isomer or when energy differences are small, modest amounts of electronic coupling cause the double minimum potential energy surface to collapse to a single minimum, corresponding to a single class III fully delocalized state. There is only one previous report of the phenomenon that we refer to here as mixed valence isomerism, and that is from earlier work from our research groups.[3] We now communicate additional observations of the existence of mixed valence isomers. These results demonstrate that the introduction of an asymmetry into a mixed valence complex by use of an asymmetric 2-methyl pyrazine (mpz) bridging ligand lifts the energy degeneracy of the two mixed valence isomers, which can then each be observed by IR spectroscopy after selective isotopic substitution. Importantly, this work establishes mixed valence isomers as discrete chemical species that exist in equilibrium. Dynamical coalescence of the observed IR line shapes further indicates that the mixed valence isomers reported here exist in dynamic equilibrium governed by electron transfers that occur on the picosecond time scale.

Ruthenium clusters of the type $[Ru_3O(\mu\text{-}CH_3COO)_6COL]\mu\text{-}L'\text{-}[Ru_3O(\mu\text{-}CH_3COO)_6COL'']$ have been of considerable interest as mixed valence complexes, since they have several easily accessible oxidation states and contain CO ligands as spectroscopic probes of the effective oxidation state at each metal cluster.[4−7] Previous work by our laboratories showed that rate constants for electron transfer in the singly reduced (mixed valence) state of the ruthenium cluster dimers can be measured by line shape analysis of coalesced ν(CO) bands in the IR spectra.[6,7] The observation of mixed valence isomers by IR spectroscopy requires an asymmetric structure of the mixed valence state and appropriate isotopic substitution to spectroscopically differentiate the two sides of the mixed valence complex. Complexes **1** and **2** (Figure 1) satisfy these criteria. The complexes were synthesized according to a modification of the established "metal complex as ligand" procedures.[8,9] The precursor trinuclear cluster, $[Ru_3O(\mu\text{-}CH3COO)_6(CO)(py)]$mpz, was synthesized as one regioisomer under kinetic control, evidenced by ^{1}H NMR spectroscopy.[10] The more basic mpz nitrogen atom (α to the methyl group) is also the more sterically hindered, so it is the less basic nitrogen that binds to the first ruthenium cluster under kinetic control. In a subsequent step, the second cluster is added and binds to the uncoordinated nitrogen atom of the mpz ligand already attached to the first cluster. In this way the two dimers, **1** and **2**, are synthesized as pure materials starting with an unlabeled CO substituted trinuclear cluster (**1**) or a $^{13}C^{18}O$ labeled cluster (**2**).

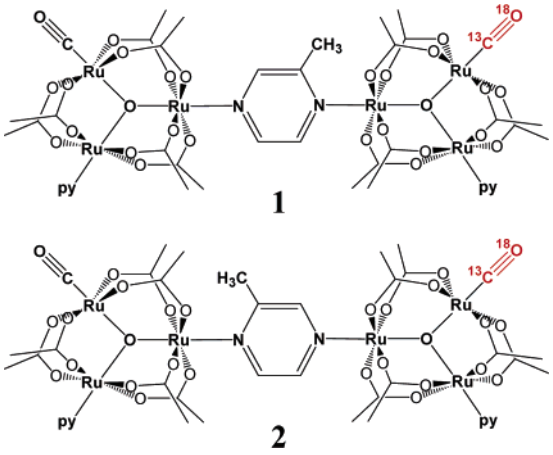

Figure 1. The two dimers synthesized for this study, differing only in location of the $^{13}C^{18}O$ label relative to the methyl group on the bridge.

Cyclic voltammetry in a 0.1 M tetrabutylammonium hexafluorophosphate solution in methylene chloride vs. the ferrocene/ferrocenium reference reveals two two-electron oxidations ($E_{1/2}$ = 200, 1000 mV) and two one-electron reductions ($E_{1/2}$ = −1160, −1500 mV). The splitting in the reduction waves, ΔE, is 340 mV and corresponds to a comproportionation equilibrium constant[11] of 5.6×10^5. The total electrochemical splitting reflects both the electronic interactions typical of a strongly electronically coupled mixed valence complex and the intrinsically different reduction potentials of the clusters bound to the different nitrogen atoms of the bridging methyl pyrazine ligand.[3,7] It will be shown that the equilibrium constants between the mixed valence isomers formed from **1** or **2** are small, and thus the electrochemical splittings observed by cyclic voltammetry are dominated by the electronic interactions. This indicates the presence of a strongly coupled mixed valence state.

Infrared spectroelectrochemistry[12] of **1** and **2** reveals exchange pairs consistent with mixed valence isomerism (Figure 2). In the case of **1** (Figure 2, left), the neutral and doubly reduced (−2) states each show two ν(CO) bands, separated by ca. 90 cm^{-1}, the intrinsic frequency separation due to the isotope substitution, $\nu(^{12}C^{16}O)$ vs $\nu(^{13}C^{18}O)$. In the mixed valence (−1) state of **1**, *four* ν(CO) bands are observed, and these correspond (from higher to lower energy) to (1) the $\nu(^{12}C^{16}O)$ contribution from the minor (less stable) mixed valence isomer, (2) the $\nu(^{12}C^{16}O)$ contribution from the major (more

10.1021/ja042351+ CCC: $30.25

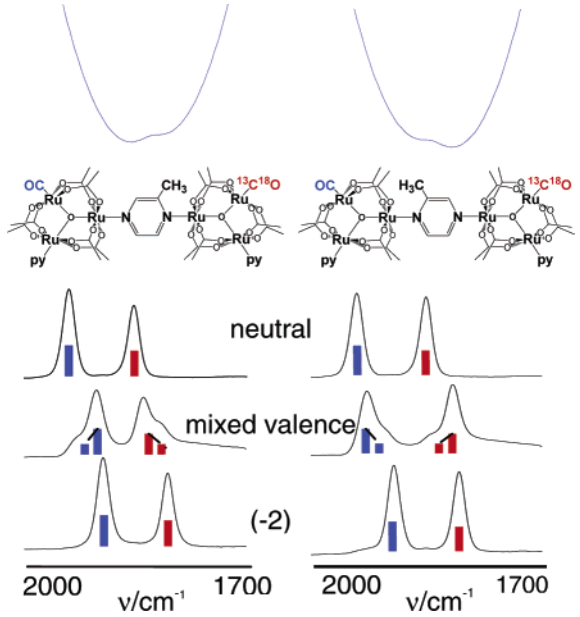

Figure 2. Infrared spectroelectrochemistry of **1** (left) and **2** (right) at −30 °C in a 0.1 M tetra-*n*-butyl ammonium hexafluorophosphate solution in CH_2Cl_2. Spectra for the neutral (top), charge transfer (middle), and doubly reduced (bottom) states are shown with a schematic of the exchanging populations. Qualitative potential energy surfaces showing the double minima of the major and minor isomer states are shown at top.

stable) mixed valence isomer, (3) the $\nu(^{13}C^{18}O)$ contribution from the major isomer, and (4) the $\nu(^{13}C^{18}O)$ contribution from the minor isomer. Note that in the mixed valence state of **1**, the spectral pattern (from higher to lower energy) corresponds to contributions from the minor, major, major, and minor isomers, while in the mixed valence state of **2**, the spectral pattern is reversed to major, minor, minor, major. This is the expected result of reversing the location of the $^{13}C^{18}O$ ligand in the asymmetric mixed valence complex. On account of the N-atom basicity differences of the mpz ligand, the minor isomer of **1** is expected to have the negative charge mostly on the cluster with the $^{13}C^{18}O$ ligand. The lowest frequency component of the overall ν(CO) spectrum is then assigned easily to the cluster of the minor isomer bearing both the negative charge and the $^{13}C^{18}O$ since both the charge and heavier isotopes shift ν(CO) to lower frequency. For similar reasons, the highest frequency part of the overall ν(CO) spectrum is assigned to the $^{12}C^{16}O$ substituted cluster of the minor isomer since ν(CO) is not perturbed by either charge or heavier isotope substitution. The remaining more intense bands in the center of the ν(CO) spectrum of the mixed valence state of **1** are assigned to the major isomer. Reversing the $^{13}C^{18}O$ substituted side of the cluster in going from **1** to **2** reverses whether each spectral component originates from the major or minor isomer. These data provide the most compelling evidence to date of the existence of mixed valence isomers as discrete chemical species. It can also be seen that both the high frequency $\nu(^{12}C^{16}O)$ and low frequency $\nu(^{13}C^{18}O)$ portions of the IR spectra of the mixed valence states are extensively coalesced exchange line shapes resulting from the dynamics of the intramolecular electron transfer between the minor and major mixed valence isomers. By using line shape simulation methods previously developed in our laboratories,[7,13] we can estimate the rate constants for electron exchange, as well as the equilibrium constant between the major and minor mixed valence isomers.

Analysis of the spectral line shapes of **1** and **2** gives an uphill rate (k_+) for charge transfer of 6.5×10^{11} s^{-1}, which compares well with previously reported rate constants for similar *symmetric* mixed valent dimers of ruthenium trinuclear clusters.[3,6] The equilibrium constant for the charge distribution (k_-/k_+) is 2.2. Future work will investigate and compare the effects of introducing other symmetrically and asymmetrically substituted bridging ligands on electron transfer rates and charge equilibria and on the factors that determine when mixed valence isomers will exist in preference to a single fully delocalized state.

Acknowledgment. This work was supported by NSF (CHE - 0315593 and INT - 0087420).

References

(1) Marcus, R. A. *J. Chem. Phys.* **1956**, *24*, 966.
(2) Hush, N. *Prog. Inorg. Chem.* **1967**, *8*, 391.
(3) Ito, T.; Imai, N.; Yamaguchi, T.; Hamaguchi, T.; Londergan, C. H.; Kubiak, C. P. *Angew. Chem., Int. Ed.* **2004**, *43*, 1376−1381.
(4) Baumann, J. A.; Salmon, D. J.; Wilson, S. T.; Meyer, T. J.; Hatfield, W. E. *Inorg. Chem.* **1978**, *17*, 3342−3350.
(5) Baumann, J. A.; Wilson, S. T.; Salmon, D. J.; Hood, P. L.; Meyer, T. J. *J. Am. Chem. Soc.* **1979**, *101*, 2916−2920.
(6) Ito, T.; Hamaguchi, T.; Nagino, H.; Yamaguchi, T.; Washington, J.; Kubiak, C. P. *Science* **1997**, *277*, 660−663.
(7) Ito, T.; Hamaguchi, H.; Nagino, H.; Yamaguchi, T.; Kido, H.; Zavarine, I. S.; Richmond, T.; Washington, J.; Kubiak, C. P. *J. Am. Chem. Soc.* **1999**, *121*, 4625−4632.
(8) Kido, H.; Nagino, H.; Ito, T. *Chem. Lett.* **1996**, 745−746.
(9) Complexes **1** and **2** were synthesized according to the strategy described in ref 8 with extra caution taken to ensure only one isomer of the precursor monomer was present. The monomer was purified by precipitation from CH_2Cl_2 by hexanes, followed by column chromatography (over silica gel; eluent 2% MeOH in $CHCl_3$), and finally gel filtration (Bio-Beads SX-3 in $CHCl_3$). The resulting dimer was purified by precipitation from CH_2Cl_2/ether only, as chromatography tended to break apart the dimer. For **1**: Anal. Calcd for $Ru_6C_{40}{}^{13}CH_{52}O_{27}{}^{18}ON_4$: C (both isotopes) 29.75; H, 3.17; N, 3.38. Found: C, 29.55; H, 3.18; N, 3.21. ^{1}H NMR (400 MHz, $CDCl_3$) 9.31 (1H, pz), 9.00 (1H, pz), 8.95 (4H, py-*ortho*), 8.92 (1H, pz), 8.14 (2H, py-*para*), 8.04 (py-*meta*), 3.25 (pz-CH_3), 2.23 (12H, acetate CH_3), 2.16 (12H, acetate CH_3), 2.00 (12H, acetate CH_3) ppm. KBr (νCO) 1950 cm^{-1}; ($\nu^{13}C^{18}O$) 1861 cm^{-1}. For **2**: Anal. Calcd for $Ru_6C_{40}{}^{13}CH_{52}O_{27}{}^{18}ON_4$: C (both isotopes) 29.75; H, 3.17; N, 3.38. Found: C, 30.34; H, 3.34; N, 3.20. ^{1}H NMR (400 MHz, $CDCl_3$) 9.31 (1H, pz), 9.00 (1H, pz), 8.95 (4H, py-*ortho*), 8.92 (1H, pz), 8.15 (2H, py-*para*), 8.05 (py-*meta*), 3.26 (pz-CH_3), 2.24 (12H, acetate CH_3), 2.15 (12H, acetate CH_3), 2.00 (12H, acetate CH_3) ppm. KBr (νCO) 1948 cm^{-1}; ($\nu^{13}C^{18}O$) 1859 cm^{-1}.
(10) For $[Ru_3O(\mu\text{-}CH_3COO)_6(CO)(py)]$mpz: ^{1}H NMR (400 MHz, $CDCl_3$) 9.07 (1H, pz), 8.97 (2H, py-*ortho*), 8.60 (1H, pz), 8.56 (1H, pz), 8.13 (1H, py-*para*), 8.00 (py-*meta*), 2.83 (3H, pz-CH_3), 2.12 (6H, acetate-CH_3), 2.09 (6H, acetate-CH_3), 1.87 (6H, acetate-CH_3). For $[Ru_3O(\mu\text{-}CH_3COO)_6(^{13}C^{18}O)(py)]$mpz: ^{1}H NMR (400 MHz, $CDCl_3$) 9.07 (1H, pz), 8.98 (2H, py-*ortho*), 8.60 (1H, pz), 8.56 (1H, pz), 8.13 (1H, py-*para*), 8.00 (py-*meta*), 2.84 (3H, pz-CH_3), 2.13 (6H, acetate-CH_3), 2.10 (6H, acetate-CH_3), 1.88 (6H, acetate-CH_3).
(11) Defined as "Ru_3O"(0) + "Ru_3O"(−2) ⇌ 2"Ru_3O"(−1). $K_c = \exp(nF\Delta E)$.
(12) Zavarine, I. S.; Kubiak, C. P. J. *Electroanal. Chem.* **2001**, 495, 106−109.
(13) McClung, R. E. D. *VibexGL: Program for the Simulation of IR Spectra of Exchanging Systems.*

JA042351+